Radiation-Corrected Open-Ended Coax Line Technique for Dielectric Measurements of Liquids up to 20 GHz

Yan-Zhen Wei and S. Sridhar

Abstract—**An experimental technique and associated analysis are described for the measurement of the dielectric constants of liquids at microwave frequencies using an open-ended coax probe. The analysis includes radiative corrections to the probe–liquid interface impedance. The technique is applicable to liquid and liquidlike (e.g., biological) samples, having dielectric constants comparable to water, at frequencies up to 20 GHz and possibly as high as 40 GHz.**

I. Introduction

An open-ended coax line affords an excellent noninvasive probe for measurements of the dielectric constants of liquids at microwave frequencies [1]–[3]. Although there have been several attempts to use such probes, experimental and analytical limitations have restricted the usable frequency range to only a few gigahertz, particularly for high ϵ' liquids such as water. The principal difficulties arising with such measurements are (1) accurate determination of the frequency-dependent probe-end impedance in vacuum, (2) elimination of spurious impedances such as those due to connector mismatch, (3) indeterminacy of probe parameters, and (4) accurate modeling of the probe–liquid interface impedance after the above problems are eliminated.

We have recently developed a technique [1] for measurements of the ϵ' and ϵ'' of liquids up to 20 GHz utilizing an ultra-small-diameter (0.047 in.) coax line dipped in the liquid. Impedances were measured using an HP8510 network analyzer with an HP8341B synthesizer. The probe–liquid interface impedance was modeled as a capacitance, and radiation effects were minimized by the use of a narrow coax probe. A new method of analysis (in terms of functions called Δ's) was developed by which, with the use of appropriate calibrations, the unknown connector impedances and such probe parameters as the fringe field capacitances $C_f, C(\omega)$ were directly eliminated. It was shown that the method could be successfully applied up to 20 GHz for several liquids.

Radiation effects become increasingly important with increasing ω, ϵ', and probe size and invalidate a simple capacitance approximation. In the absence of a good model incorporating such effects, we previously [1] adopted an empirical approach to minimizing these effects by using the narrowest convenient probe, viz. a 0.047 in. coax line and retaining a capacitance approximation. While this approximation is quite adequate for moderate ϵ' liquids, such as methanol, the procedure is less accurate for a high ϵ' liquid such as water at higher frequencies, leaving a systematic residual uncertainty for $\omega/2\pi > 10$ GHz. In this paper, we present a complete analysis incorporating radiation effects; Marcuvitz's expression for the admittance of an open-ended coax line terminated by vacuum, is used, together with Deschamps's theorem to include the dielectric permittivity of the medium, which removes the residual uncertainty at high frequencies. Although the use of the narrow coax itself minimizes the radiation effects and allows the application of Marcuvitz's approximation as a correction, the analysis presented here greatly improves the accuracy of the deduced $\epsilon(\omega)$ values.

In previous work [2] by Kraszewski *et al.*, where calibrations were used to account for transmission discontinuities in the line, the analysis relied on a knowledge of the probe-end capacitances. Consequently, the data range was limited to 5 GHz for water. Recent work [3] by Misra *et al.* does consider radiation effects. However, because of the use of a larger probe (3.6 mm), the approximation made by using Marcuvitz's expressions for the probe-end impedance, while improving the methanol results from 1 to 18 GHz, is valid only up to about 10 GHz for water and appears to break down at higher frequencies (> 10 GHz) since the ϵ' of water is about one order of magnitude greater than that of methanol. Higher frequencies are essential for aqueous samples, since the dielectric relaxation frequency of water is about 17 GHz at ambient temperatures. Our approach [1], which takes into account all of the factors mentioned earlier through a different method of analysis and a narrow probe, thereby making Marcuvitz's approximation applicable to higher frequencies, is significantly more accurate than previously possible.

Manuscript received February 5, 1990; revised July 9, 1990. This work was supported by the Petroleum Research Fund of the American Chemical Society.

The authors are with the Department of Physics, Northeastern University, Boston, MA 02115.

IEEE Log Number 9041964.

II. Description of the Technique

The measurement configuration (Fig. 1) consists of a narrow (0.047 in.) coax line cut flat at one end which is dipped into the liquid. To the other end is attached an SMA

0018-9480/91/0300-0526$01.00 ©1991 IEEE

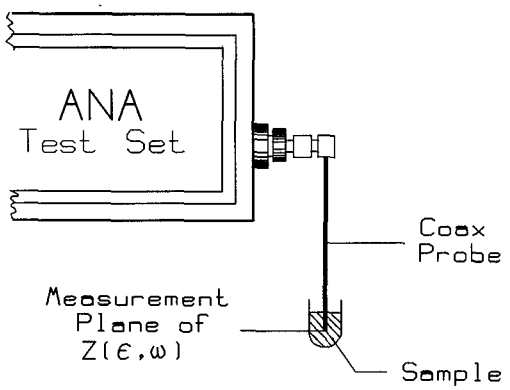

Fig. 1. Measurement configuration.

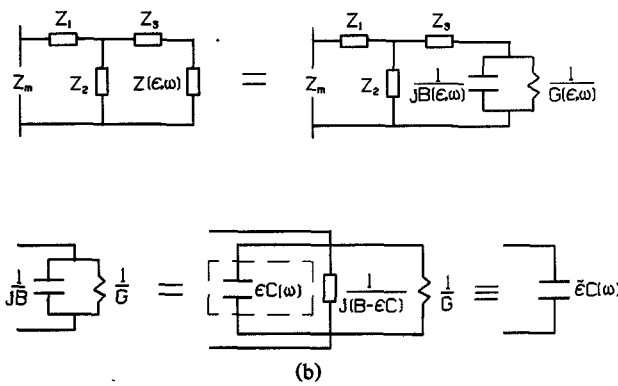

Fig. 2. Equivalent circuit for the measurement configuration. (a) The T-network representation used in this work. The impedances Z_i ($i = 1,2,3$) include line discontinuities, such as connector impedances and also the probe capacitance. Z_m is the impedance seen by the ANA at its measurement plane. Z is the impedance of the probe–liquid interface. All elements of the figure are complex quantities. (b) Elements of the probe–liquid impedance, including radiation corrections. The element ϵC enclosed in the box represents a simple capacitance approximation used in earlier work, while the remaining elements describe the radiation correction.

connector which is then connected to an HP8510B network analyzer. The synthesized source (HP8341B) was used in the step mode for higher accuracy. Pairwise reflection coefficient data were collected for the sample liquid and three calibrations [open, a short (liquid Hg), and a standard liquid such as acetone]. The calibration process locates the measurement plane at the coax end. The transmission line from the ANA plane to the coax end plane, including connector and line impedances and probe fringe capacitance, was modeled as a T network with impedances Z_1, Z_2 and Z_3 (see Fig. 2(a)). The three calibrations eliminate these three impedances, and from the fourth sample measurement the probe–liquid interface impedance $Z(\omega,\epsilon)$ is determined.

In our earlier work [1], the coax–liquid impedance was modeled as a simple capacitance $Z(\omega,\epsilon) = 1/Y(\omega,\epsilon) = 1/j\omega C\epsilon$. For a complex $C(\omega)$ and ϵ, the equivalent circuit is only a dissipative capacitor, shown in Fig. 2(b) enclosed in the dashed rectangular box. In [1], the analysis of the data from which $\epsilon(\omega)$ was inferred is described in detail for the above model. In this paper, we include radiation effects in the model for $Z(\omega,\epsilon)$ and describe the analysis to deduce $\epsilon(\omega)$ from a similar set of four measurements.

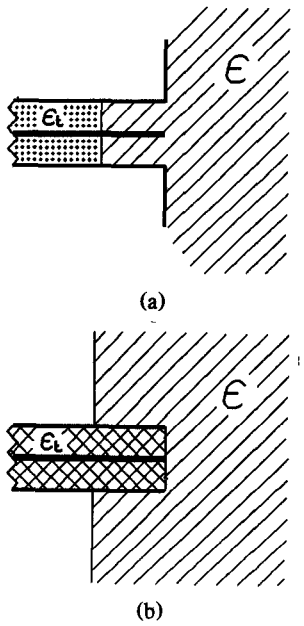

Fig. 3. (a) Configuration for Deschamps's theorem. (b) Actual configuration used in this work.

III. Radiation-Corrected Theory of Open Ended Coax Line Dipped in a Liquid

The fringe admittance of a vacuum-filled flanged open-ended coax probe that opens to a half free space can be represented generally as

$$Y_v(\omega, \epsilon = 1) = G_v(\omega, \epsilon = 1) + jB_v(\omega, \epsilon = 1). \quad (1)$$

Marcuvitz [4] expressed G_v and B_v as

$$G_v = \frac{Y_{v0}}{\ln(a/b)} \cdot \int_0^{(\pi/2)} \frac{1}{\sin\theta} \left[J_0(k_0 a \sin\theta) - J_0(k_0 b \sin\theta)\right]^2 d\theta \quad (2)$$

$$B_v = \frac{Y_{v0}}{\pi \ln(a/b)} \int_0^{\pi} \left\{2\,\mathrm{Si}\left[k_0\sqrt{(a^2+b^2-2ab\cos\theta)}\right] - \mathrm{Si}\left[2k_0 a \sin(\theta/2)\right] - \mathrm{Si}\left[2k_0 b \sin(\theta/2)\right]\right\} d\theta. \quad (3)$$

Here a and b denote the outer and inner radii of the line, $k_0 = \omega/c$ is the wavenumber in vacuum, and Y_{v0} is the characteristic admittance of the line. Deschamps [5] pointed out that the admittance of the vacuum-filled probe open to a medium of ϵ, $\mu = 1$, as depicted in Fig. 3(a), can be shown to be

$$Y_a(\omega,\epsilon) = \sqrt{\epsilon}\, Y_{av}(\sqrt{\epsilon}\,\omega, 1) \quad (4)$$

where Y_{av} is the admittance of the probe open to the free space. Now the radiation from a Teflon-filled coax with characteristic admittance Y_0 is equivalent to that from a vacuum-filled coax of the same size but with characteristic admittance $Y_0/\sqrt{\epsilon_t}$, where ϵ_t is the dielectric constant of Teflon. If the vacuum-filled coax in Fig. 3(a) is replaced by a Teflon-filled coax, the admittance Y_a' would be

$$Y_a'(\omega,\epsilon) = \sqrt{\epsilon}\, Y_{av}(\sqrt{\epsilon}\,\omega, 1)/\sqrt{\epsilon_t}. \quad (5)$$

The configuration of interest here is an open-ended Teflon-filled semirigid coax probe dipped into a liquid, as shown in Fig. 3(b). There are two minor differences from the configuration Fig. 3(a). First, the free-space probe-end admittance is different from $Y_v(\omega,1)$ obtained from (1)–(3), owing to the absence of the flange. Second, Deschamps's theorem is only approximately valid for this configuration. Here we introduce a frequency-dependent configuration function of probe parameters a, b, and ϵ_t, viz. $\alpha(a,b,\omega,\epsilon_t)$, which represents the medium-independent modifications to the admittance, when applying Deschamps's theorem to Marcuvitz's expression in the configuration of Fig. 3(b). Hence the probe-end admittance of the Teflon-filled flat-end coax surrounded by a liquid is approximated as

$$Y(\omega,\epsilon)=[G(\omega,\epsilon)+jB(\omega,\epsilon)]=\alpha(a,b,\omega,\epsilon_t)Y_b' \quad (6)$$

where

$$Y_b'=\sqrt{\epsilon}\,Y_v(\sqrt{\epsilon}\,\omega,1)\Big/\sqrt{\epsilon_t}\,. \quad (7)$$

Using (2) and (3),

$$G=\frac{\alpha Y_0\sqrt{\epsilon}}{\ln(a/b)\sqrt{\epsilon_t}}\cdot\int_0^{(\pi/2)}\frac{1}{\sin\theta}\left[J_0\left(k_0\sqrt{\epsilon}\,a\sin\theta\right)-J_0\left(k_0\sqrt{\epsilon}\,b\sin\theta\right)\right]^2 d\theta \quad (8)$$

$$B=\frac{\alpha Y_0\sqrt{\epsilon}}{\pi\ln(a/b)\sqrt{\epsilon_t}}\cdot\int_0^{\pi}\Big\{2\,\mathrm{Si}\left[k_0\sqrt{\epsilon(a^2+b^2-2ab\cos\theta)}\right]-\mathrm{Si}\left[2k_0\sqrt{\epsilon}\,a\sin(\theta/2)\right]-\mathrm{Si}\left[2k_0\sqrt{\epsilon}\,b\sin(\theta/2)\right]\Big\}d\theta. \quad (9)$$

If we expand the integrals in the two above expressions in powers of $k_0\sqrt{\epsilon}=\gamma$:

$$G(\omega,\epsilon)=\alpha\sqrt{\epsilon}\cdot\left(g_1\gamma^2+g_2\gamma^4+g_3\gamma^6+\cdots+g_k\gamma^{2k}+\cdots\right)\Big/\sqrt{\epsilon_t} \quad (10)$$

$$B(\omega,\epsilon)=\alpha\sqrt{\epsilon}\cdot\left(b_1\gamma+b_2\gamma^3+b_3\gamma^5+\cdots+b_k\gamma^{2k-1}+\cdots\right)\Big/\sqrt{\epsilon_t} \quad (11)$$

we can write

$$Y=G+jB\equiv j\omega C(\omega)\tilde{\epsilon}(\omega,\epsilon) \quad (12)$$

where

$$C(\omega)\equiv\alpha b_1\Big/\left(c\sqrt{\epsilon_t}\right) \quad (13)$$

is the fringe-field capacitance due to the electric field outside the probe. The quantity $j\omega C$ can be regarded as the exact coefficient of the lowest order expansion of $Y(\omega,\epsilon)$ in powers of $\sqrt{\epsilon}$ for the semirigid coax probe dipped into a liquid medium. In general, this could be different from that calculated from the lowest order expansion of (6) because of the differences between the two measurement configurations in Fig. 3. As we shall see later, the detailed functional form of α is not important, as it gets eliminated. From (12),

$$\tilde{\epsilon}\equiv(G+jB)\big/j\omega C. \quad (14)$$

Substituting

$$Z(\omega,\epsilon)=\frac{1}{Y(\omega,\epsilon)}\equiv\frac{1}{G+jB}=\frac{1}{j\omega C\tilde{\epsilon}} \quad (15)$$

into [1, eqs. (9)–(12)], we obtain

$$\Delta+\frac{\Delta_{12}}{\tilde{\epsilon}_A}+\Delta_{23}Z_{MA}=\frac{Z_{MA}}{\tilde{\epsilon}_A} \quad (16)$$

$$\Delta+\frac{\Delta_{12}}{\tilde{\epsilon}_B}+\Delta_{23}Z_{MB}=\frac{Z_{MB}}{\tilde{\epsilon}_B} \quad (17)$$

$$\Delta+\frac{\Delta_{12}}{\tilde{\epsilon}_C}+\Delta_{23}Z_{MC}=\frac{Z_{MC}}{\tilde{\epsilon}_C} \quad (18)$$

$$\Delta+\frac{\Delta_{12}}{\tilde{\epsilon}}+\Delta_{23}Z_M=\frac{Z_M}{\tilde{\epsilon}} \quad (19)$$

where the Δ's are functions of Z_1, Z_2 and Z_3 (see Fig. 2(a)) and the $\tilde{\epsilon}$'s are obtained from (14) for different media surrounding the probe end. We can further rearrange the equations by substituting

$$Z_i=Z_0\frac{1+\rho_i}{1-\rho_i}\quad(i=MA,MB,MC,M) \quad (20)$$

where $\rho_i=\Gamma_i e^{j\phi_i}$ is the reflection coefficient of the open ($i=MA$), short ($i=MB$), standard liquid ($i=MC$), or sample liquid ($i=M$) from the probe end, into the above four equations with a new set of Δ's:

$$\Delta+\Delta_{12}\tilde{\epsilon}_A+\Delta_{23}\rho_{MA}=\tilde{\epsilon}_A\rho_{MA} \quad (21)$$

$$\Delta+\Delta_{12}\tilde{\epsilon}_B+\Delta_{2e}\rho_{MB}=\tilde{\epsilon}_B\rho_{MB} \quad (22)$$

$$\Delta+\Delta_{12}\tilde{\epsilon}_C+\Delta_{23}\rho_{MC}=\tilde{\epsilon}_C\rho_{MC} \quad (23)$$

$$\Delta+\Delta_{12}\tilde{\epsilon}+\Delta_{23}\rho_M=\tilde{\epsilon}\rho_M. \quad (24)$$

From here we see that the $\tilde{\epsilon}$'s and ρ's satisfy

$$\frac{(\tilde{\epsilon}-\tilde{\epsilon}_A)(\tilde{\epsilon}_B-\tilde{\epsilon}_C)}{(\tilde{\epsilon}-\tilde{\epsilon}_B)(\tilde{\epsilon}_C-\tilde{\epsilon}_A)}=\frac{(\rho_M-\rho_{MA})(\rho_{MB}-\rho_{MC})}{(\rho_M-\rho_{MB})(\rho_{MB}-\rho_{MA})}. \quad (25)$$

It can be also shown that if (12) is substituted into the alternative formulation of an S-parameter description of the microwave network, i.e.,

$$\frac{(Y-Y_A)(Y_B-Y_C)}{(Y-Y_B)(Y_C-Y_A)}=\frac{(\rho_M-\rho_{MA})(\rho_{MB}-\rho_{MC})}{(\rho_M-\rho_{MB})(\rho_{MC}-\rho_{MA})} \quad (26)$$

which applies to the case of the reference plane "sitting" between the fringe field C_f due to the electric field inside the coaxial line and $C(\omega)$, the result given by (25) is obtained. This shows the equivalence of an S-parameter description to the "lumped" circuit description of this work.

IV. Results

The algorithm for the numerical analysis of the data is shown as a flow graph in Fig. 4. The expressions (10) and (11) for G and B were expanded to the 31st power of γ (most terms can be found from [3] and [6]). The coefficients g_i and b_i were calculated using an IBM PC. They were transferred to a VAX to calculate the coefficients of the

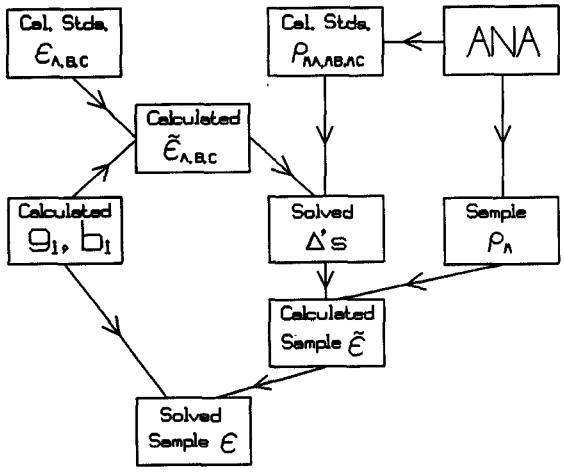

Fig. 4. Flow diagram for the numerical algorithm used to extract dielectric coefficients ϵ from measured reflection coefficients ρ_M.

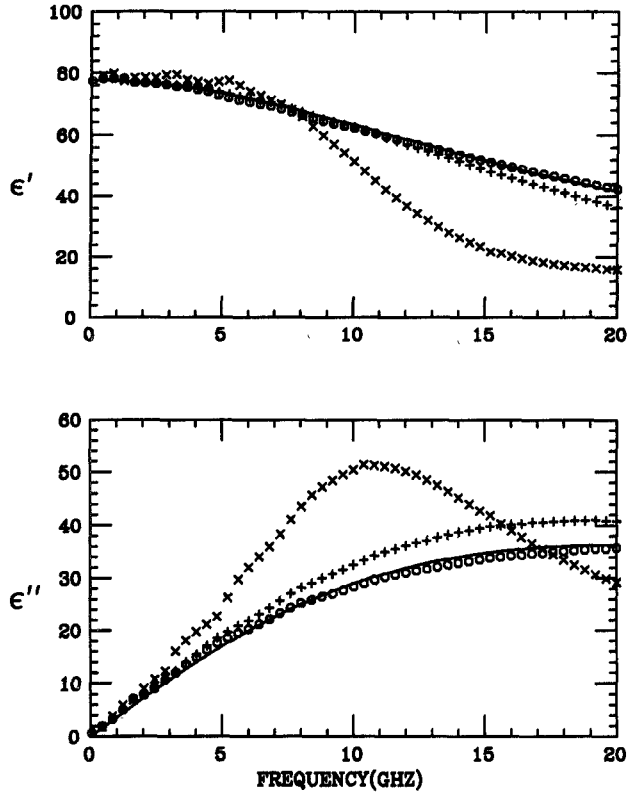

Fig. 5. Results for ϵ' and ϵ'' for water between 45 MHz and 20 GHz. O: radiation corrected results for 0.047 in probe, +: uncorrected results for 0.047 in. probe. Also displayed are uncorrected results using a 0.141 in. probe (×'s), showing the large errors caused by radiation with increasing probe size. The solid line represents a Debye fit to the corrected 0.047 in. results.

complex polynomial $\tilde{\epsilon}(\omega,\epsilon)$. Then $\tilde{\epsilon}(\omega,\epsilon)$ was found for the open, the short, and the standard liquid acetone, viz. $\tilde{\epsilon}_A$, $\tilde{\epsilon}_B$, and $\tilde{\epsilon}_C$, respectively. The polynomial $\tilde{\epsilon}(\omega,\epsilon)$ of deionized water as a sample was then obtained from the three sets of calibration data, the reflection coefficient ρ_M of the water samples, and $\tilde{\epsilon}_A$, $\tilde{\epsilon}_B$, and $\tilde{\epsilon}_C$ (see Fig. 4). A zero-finding program from IMSL was used to solve the dielectric constant ϵ of the sample from $\tilde{\epsilon}(\omega,\epsilon)$ as expressed in (14), (7), and (8).

The radiation-corrected data of water, deduced from the measurements using a 0.047 in. probe and the analysis described above, are plotted in Fig. 5. Also shown are uncorrected results for a 0.047 in. probe and for a larger, 0.141 in. probe, obtained using the capacitance approximation of [1]. For ϵ', it is evident from Fig. 5 that the correction is small ($\delta\epsilon'/\epsilon' < 3\%$) at $\omega/2\pi < 12$ GHz and only slightly larger for higher frequencies, reaching $\delta\epsilon'/\epsilon' = 10\%$ for 20 GHz. The corrections are larger for ϵ'' viz., $\delta\epsilon''/\epsilon'' < 10\%$ up to 12 GHz and 12% at 20 GHz. It is important to remember that this is only true for the 0.047 in. probe. For larger probes, the radiation effects are much greater, as may be seen from Fig. 5.

The corrected data can be fit to a Debye curve with $\epsilon_0 = 77.6$, $\epsilon_\infty = 5.0$, and $\tau = 7.9$ ps (at the measurement temperature $T = 27°C$), exhibited as the solid line in Fig. 4. These parameters are more accurate than without the radiation correction [1]. Thus the measurement allows the observation of the complete relaxation spectrum of water.

V. Error Analysis

We next discuss the errors arising from two sources: (1) random errors introduced by the measurements and (2) errors arising from inaccuracies in the calibration data. The limitations of the coax-end impedance modeling, which are at present difficult to quantify, are discussed in the next section.

Experimentally we find that the largest errors (called $d\rho_M$) introduced in the measurements of the reflection coefficients ρ_M, are caused by long-term drift of the ANA, and are of the order $|\delta\rho_M/\rho_M| \sim 1\%$. The actual accuracy of the machine (e.g., for measurements of an impedance at the terminal plane of the test set) as stated by the manufacturer is much greater, with errors of order 0.1%; hence we ignore them and consider only the long-term drift contributions.

Inaccuracies in the values assumed for the calibrations, viz. the open, the short, and the acetone standard, could also introduce errors in the deduced ϵ values. The open calibration, done without any liquid, is taken to correspond to $\epsilon_A = 1$. The short, carried out using liquid Hg, is also accurate and corresponds to $\epsilon_B'' \to \infty$. In the following we examine the possible effect of inaccuracies in the assumed values for the acetone standard, i.e., a possible error of $|\delta\epsilon_C'/\epsilon_C'| = |\delta\epsilon_C''/\epsilon_C''| = 2\%$ at all frequencies in ϵ_C for which we have assumed a Debye form.

Taking the derivative of (25), we get

$$
\begin{aligned}
&-\frac{\tilde{\epsilon}_B-\tilde{\epsilon}_A}{(\tilde{\epsilon}-\tilde{\epsilon}_B)(\tilde{\epsilon}-\tilde{\epsilon}_A)}d\tilde{\epsilon}+\frac{\tilde{\epsilon}-\tilde{\epsilon}_C}{(\tilde{\epsilon}_A-\tilde{\epsilon})(\tilde{\epsilon}_A-\tilde{\epsilon}_C)}d\tilde{\epsilon}_A\\
&-\frac{\tilde{\epsilon}-\tilde{\epsilon}_C}{(\tilde{\epsilon}_B-\tilde{\epsilon})(\tilde{\epsilon}_B-\tilde{\epsilon}_C)}d\tilde{\epsilon}_B+\frac{\tilde{\epsilon}_B-\tilde{\epsilon}_A}{(\tilde{\epsilon}_C-\tilde{\epsilon}_B)(\tilde{\epsilon}_C-\tilde{\epsilon}_A)}d\tilde{\epsilon}_C\\
&=-\frac{\rho_{MB}-\rho_{MA}}{(\rho_M-\rho_{MB})(\rho_M-\rho_{MA})}d\rho_M\\
&\quad+\frac{\rho_M-\rho_{MC}}{(\rho_{MA}-\rho_M)(\rho_{MA}-\rho_{MC})}d\rho_{MA}\\
&\quad-\frac{\rho_M-\rho_{MC}}{(\rho_{MB}-\rho_M)(\rho_{MB}-\rho_{MC})}d\rho_{MB}\\
&\quad+\frac{\rho_{MB}-\rho_{MA}}{(\rho_{MC}-\rho_{MB})(\rho_{MC}-\rho_{MA})}d\rho_{MC}
\end{aligned}
\tag{27}
$$

TABLE I
CALCULATED ERRORS AND MEASURED STANDARD DEVIATION OF ϵ' AND ϵ''

	Machine[a]		Acetone[b]		Standard Deviation[c]	
f (GHz)	$\delta\epsilon'/\epsilon'$	$\delta\epsilon''/\epsilon''$	$\delta\epsilon'/\epsilon'$	$\delta\epsilon''/\epsilon''$	$\delta\epsilon'/\epsilon'$	$\delta\epsilon''/\epsilon''$
0.045	> 0.30	> 0.30	0.02	< 0.005	0.06	> 1.00
1	0.25	0.25	0.02	0.01	0.01	0.05
5	0.05	0.06	0.02	0.01	0.01	0.03
10	0.04	0.04	0.02	0.01	0.003	0.02
15	0.03	0.04	0.02	0.01	0.01	0.02
20	0.02	0.02	0.02	0.01	0.01	0.01

[a]Calculated assuming a 1% shift of measured reflection coefficients, constant at all frequencies.
[b]Calculated assuming a 2% error, constant at all frequencies, in the assumed values for the standard.
[c]Experimental standard deviation determined from five sets of measurements.

where $d\rho_M$, $d\rho_{MA}$, $d\rho_{MB}$, and $d\rho_{MC}$ come from the instability of the ANA during the measurements and $d\tilde{\epsilon}_A$, $d\tilde{\epsilon}_B$, and $d\tilde{\epsilon}_C$ are errors from the accepted dielectric constant of calibration standards. Substituting the open and short values of $|\epsilon_B| \to \infty$ and $\epsilon_A = 1$, the above equation is simplified as

$$d\tilde{\epsilon} = \frac{\tilde{\epsilon} - \tilde{\epsilon}_A}{\tilde{\epsilon}_C - \tilde{\epsilon}_A} d\tilde{\epsilon}_C + (\tilde{\epsilon} - \tilde{\epsilon}_A)\left[- \frac{\rho_{MB} - \rho_{MA}}{(\rho_M - \rho_{MB})(\rho_M - \rho_{MA})} d\rho_M + \frac{\rho_M - \rho_{MC}}{(\rho_{MA} - \rho_M)(\rho_{MA} - \rho_{MC})} d\rho_{MA} - \frac{\rho_M - \rho_{MC}}{(\rho_{MB} - \rho_M)(\rho_{MB} - \rho_{MC})} d\rho_{MB} + \frac{\rho_{MB} - \rho_{MA}}{(\rho_{MC} - \rho_{MB})(\rho_{MC} - \rho_{MA})} d\rho_{MC} \right]. \quad (28)$$

In Table I, we show the possible errors induced by the drift of the machine, taken to be $|\delta\rho_M/\rho_M| = 1\%$, *constant* at all frequencies. Also shown are the errors induced by an error of $|\delta\epsilon_C'/\epsilon_C'| = |\delta\epsilon_C''/\epsilon_C''| = 2\%$, also constant at all frequencies, in the assumed standard liquid ϵ_C values. The third pair of columns in Table I lists the standard deviation obtained from a set of five actual measurements, the variation being due to drifts in the machine.

One observation that is evident from Table I is that although the errors are quite acceptable for frequencies above a few 100 MHz, they are unacceptably large at the lowest frequencies, 45 MHz to about 200 MHz. The primary reason for this is the small probe size, which is inappropriate for the lower frequencies owing to the following three features: (a) the fringe field capacitance of the 0.047 in. probe is too small, so that at low ω the probe impedance is too large; (b) at low ω the reflection coefficient of the acetone calibration is too close to that of the open; and (c) at low ω, the ϵ'' of water is small. The calibration problem could be circumvented by the use of a different standard close to 50 Ω, such as a saline solution, for which, however, the ϵ_C values are not well known.

The above discussion points to the fact that in order to minimize radiation effects at high ω, one gives up accuracy at low ω. Thus the 0.047 in. probe is best used at frequencies > 500 MHz for liquids such as water. For lower frequencies, it is better to use much larger probes with greater $C(\omega)$; as is well known, there are fewer measurement problems at low ω anyway.

VI. DISCUSSION AND CONCLUSIONS

The "lumped" T circuit model used here gives a complete description of the microwave measurement system. It is simply another way of defining the linear response of the microwave network with a set of parameters different from S parameters. The mathematical equivalence between them has been demonstrated in (25) and (26).

In this work, we have gone beyond a simple capacitance approximation to the coax–liquid impedance by including radiation effects. Essential to the approach is the experimental minimization of such effects by the use of a very narrow probe, allowing the treatment of these effects as corrections. We next examine the nature of the radiation treatment considered here.

As discussed earlier, the experimental geometry does not exactly correspond to that considered by Deschamps [5]. In our treatment the effect of these differences is represented as $Y = \alpha Y_b'$. Note that the detailed functional form of α, which depends on probe dimensions a and b, and frequency f, is not important, since α cancels out in the process of analysis. This factor is included primarily to account for the absence of the outer screening conductor in Fig. 3(b) compared with Fig. 3(a). The absence of this conductor should reduce the effective capacitance from that calculated from the first term of Y_a', and this is in agreement with experiments by Li *et al.* [6] and Kraszewski, *et al.* [7]. In general the applicability of the above approximation will be limited by increasing a, b, and f. The radiation contribution to the impedance is greatly minimized for the narrow 0.047 in. probe because at $f = 20$ GHz, the wavelength in the liquid $\lambda \sim 1.5 \text{ cm}/\sqrt{\epsilon'}$, which gives the ratio of the probe aperture and the wavelength $2a/\lambda \sim 0.06/\sqrt{\epsilon'}$. This smaller value improves the validity of the approach here. From the results of [7], we estimate that for a 0.141 in. probe, $\alpha < 0.845(1 + 0.25 \times 10^{-3} f^2)$, where f is in GHz, which ranges from 0.845 to 0.95 between 45 MHz and 20 GHz. The correction would be much less for the 0.047 in. probe used in the present work.

As noted previously, the detailed form of the dependence of α on a, b, and ω is not important. However, our treatment does not account for a possible ϵ dependence of α.

The other approximation made in applying Deschamps's theorem is the neglect of higher order modes beside the TEM mode, which would be excited in the configuration of Fig. 3(b). The actual contribution of such terms is difficult to estimate. However it may be noted that the arbitrariness of the factor α means that all terms linear in Y_b' are included in the present analysis.

The radiation correction is not required for all liquids in the frequency range from 45 MHz to 20 GHz, as we have already shown in [1]. We examine the magnitude of the radiation correction for various values of ϵ' and its dependence on frequency in Fig. 6. The correction is evaluated as

$$\delta\tilde{\epsilon}'/\epsilon = \frac{\tilde{\epsilon}' - \epsilon'}{\epsilon} \qquad \delta\tilde{\epsilon}''/\epsilon = \frac{\tilde{\epsilon}'' - \epsilon''}{\epsilon} \quad (29)$$

where $\tilde{\epsilon} = \tilde{\epsilon}' - j\tilde{\epsilon}''$ for hypothetical liquids with $\epsilon = \epsilon' = 10$,

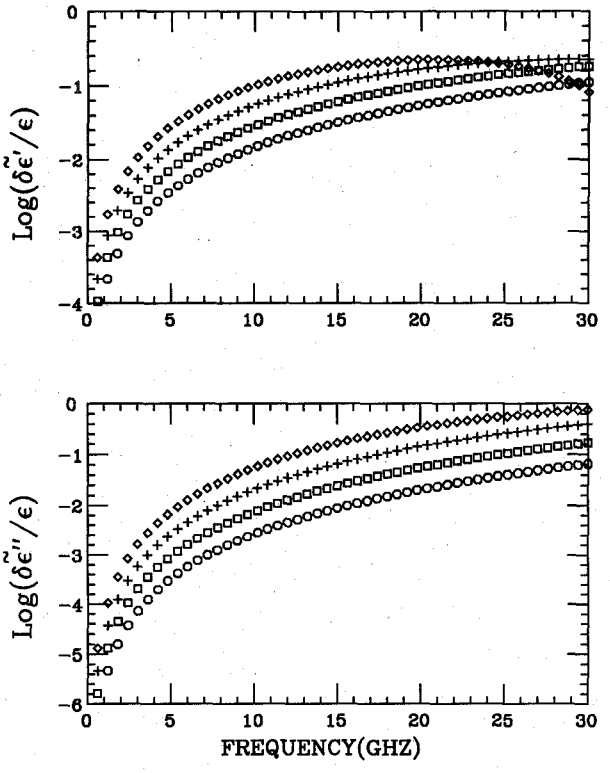

Fig. 6. Calculated magnitudes of the radiation correction, using a 0.047 in. probe, for hypothetical liquids with $\epsilon = \epsilon' = 10$ (O's), 20 (squares), 40 (+'s), 80 (diamonds), constant up to 30 GHz.

20, 40, and 80 and *independent of frequency* up to 30 GHz, and for a 0.047 in. probe. A clear feature of Fig. 6 is the strong ω dependence, with the correction negligible at low frequency but becoming increasingly important with increasing ω. For $\epsilon = 10$, the expected relative errors shown in Fig. 6 are less than 5% for the real part; for the imaginary part they are less than 2% for $\omega/2\pi < 20$ GHz. Therefore for liquids such as methanol, toluene, and methylene chloride, whose dielectric constant is less than 10 at GHz frequencies, no radiation correction is required up to 20 GHz. With increasing ϵ', the correction becomes increasingly important with frequency. (The curve for $\epsilon' = 80$ also illustrates that the first-order correction considered here is oscillatory.)

In conclusion we have presented an experimental method and analysis, including radiative effects, for a technique to measure dielectric constants of liquids at gigahertz frequencies. The technique is applicable to liquid and liquidlike samples having ϵ' values comparable to that of water and is valid to frequencies as high as 40 GHz with the use of very narrow probes. Elsewhere, we have described several results obtained using these techniques for a variety of aqueous systems [8], [9].

Acknowledgment

The authors thank G. Michel for assistance with the numerical analysis and A. Schatzberg and C. Rappaport for useful discussions.

References

[1] Y. Z. Wei and S. Sridhar, "Technique for measuring complex dielectric constants of liquids up to 20 GHz," *Rev. Sci. Instrum.*, vol. 60, no. 9, pp. 3041–3046, 1989.

[2] A. Kraszewski, M. A. Stuchly, and S. S. Stuchly, "ANA calibration method for measurement of dielectric properties," *IEEE Trans. Instrum. Meas.*, vol. IM-32, pp. 385–387, 1983.

[3] D. Misra, M. Chabbra, B. R. Epstein, M. Mirotznik and K. R. Foster, "Noninvasive electrical characterization of materials at microwave frequencies using an open-ended coaxial line," *IEEE Trans. Microwave Theory Tech.*, vol. 38, pp. 8–14, Jan. 1990.

[4] N. Marcuvitz, *Waveguide Handbook*. New York: McGraw-Hill, 1951, pp. 213–216.

[5] G. A. Deschamps, "Impedance of an antenna in a conducting medium," *IEEE Trans. Antennas Propagat.*, vol. AP-10, pp. 648–650, 1962.

[6] D. M. Xu, L. P. Liu, and Z. Y. Jiang, "Measurement of the dielectric properties of biological substances using an improved open-ended coaxial line resonator method," *IEEE Trans. Instrum. Meas.*, vol. IM-35, pp. 13–18, 1986.

[7] A. Kraszewski and S. S. Stuchly, "Capacitance of open-ended dielectric-filled coaxial lines—Experimental results," *IEEE Trans. Instrum. Meas.*, vol. IM-32, pp. 517–519, 1983.

[8] Yan-Zhen Wei and S. Sridhar, "Dielectric spectroscopy of $LiCl/H_2O$ solutions," *J. Chem. Phys.*, vol. 92, no. 2, pp. 923–928, 1990.

[9] Y. Z. Wei and S. Sridhar, W. D. Tian, and P. Champion, "Gigahertz dielectric spectroscopy: A probe of biomolecule dynamics in solutions," *Bull. Amer. Phys. Soc.* vol. 35, no. 3 p. 776, 1990.

Yan-Zhen Wei was born in Beijing, People's Republic of China, in 1962. She received the B.S. degree in physics from the Peking University, Beijing, China, in 1983 and the M.S. degree in physics from the Institute of Physics, Chinese Academy of Sciences, in 1986. She is currently a Ph.D. candidate in physics at Northeastern University, Boston, MA, where her research focuses on the dielectric properties at gigahertz frequencies of liquids and solids.

S. Sridhar received the Ph.D. degree in physics in 1983 from the California Institute of Technology. His Ph.D. thesis was on the microwave properties of superconductors.

He was a Research Fellow at Caltech in 1983 and 1984 and Adjunct Assistant Professor and Research Fellow at UCLA between 1984 and 1986. Since 1986 he has been an Assistant Professor in the Department of Physics at Northeastern University, Boston, MA. His research interests are primarily in fundamental and applied aspects of superconductivity, superconducting devices, and dielectric and conductivity properties at RF to mm-wave frequencies in liquids and solids. He presently serves on Committee MTT-18 (Microwave Superconductor Applications) of IEEE/MTT.